Parametric Identification of Postural Control Models in Humans Challenged by Impulse-Controlled Perturbations

Parametric Identification of Postural Control Models in Humans Challenged by Impulse-Controlled Perturbations

tion between physiological systems that contribute to the balance makes the interpretation of experimental results difficult. In this sense, model-based analyses [8,14–17] could be a helpful tool to achieve information about not easily monitored variables, such as joint angles and torques. Generally, human stance is modelled as a single-link inverted pendulum (SIP) pivoting on the ankle. Healthy subjects standing on a stable surface, in fact, prefer the ankle strategy to recover or maintain balance. On the other hand, the adopted strategy also depends on the previous experience of the subject and the entity of the disturbance, therefore ankle and hip strategies may be both present in postural control, with one dominating the other. In this regard, a double-link inverted pendulum (DIP) could provide additional information and more realistic kinematic result about postural response with respect to the single-link model.

This work aims to present the parametric identification of SIP and DIP models based on experimental data collected during dynamic posturography trials. These analyses have been possible thanks to a custom-made automatic device used to perturb balance in healthy subjects with appropriate control of the magnitude and duration of the perturbations. The aim of this study is to provide customizable and robust models that can help in the investigation of the mechanisms underlying postural control.

2 Materials and Methods

2.1 Experimental trials with automated perturbation device

Posturographic analyses have been conducted on 11 healthy subjects (age = 22.82 ± 2.18 years; weight = 62.45 ± 9.50 kg; height = 171 ± 11 cm; BMI = 21.36 ± 1.76 kg/m^2) with a custom-made prototype of an automated perturbation device (AP). Each analysis consisted in multiple perturbations with selectable impulse (i.e., time integral of the force profile) exerted to the back of the subject at a defined location between the scapulae. Due to prior research, two impulse levels, 6 Ns and 10 Ns, were considered to elicit responses of different amplitudes without running into the risk for falling or evoking step responses in any subject. The two levels were obtained by fixing the magnitude of the perturbation force at 40 N and by changing its duration between 150 ms and 250 ms. Each subject was standing on a force platform and faced in the opposite direction with respect to the operator handling the AP, to ensure the unpredictability of the perturbation. The signals recorded by the force platform were processed to estimate the center of pressure (CoP) displacement over the base of support.

The perturbation device (Fig. 1d, [10]) consisted of a double-acting linear pneumatic actuator controlled by two flow-proportional valves and was directly handled by a human operator. The accuracy, repeatability and scalability of the perturbations enabled by the device have already been discussed in previous works and proved to be adequate for this application [10,11]. Examples of the force and CoP signals obtained during a session with a 10 Ns impulse reference are shown in Fig. 1a-b, along with a scheme of a typical trial set-up (Fig. 1c). The signals were digitally filtered (Butterworth low-pass filter, 8th order − 150 Hz cut-off frequency for the force signal, 4th order − 20 Hz for the CoP) and segmented in order to get a consistent set of data that included 5 consecutive perturbations at each impulse level.

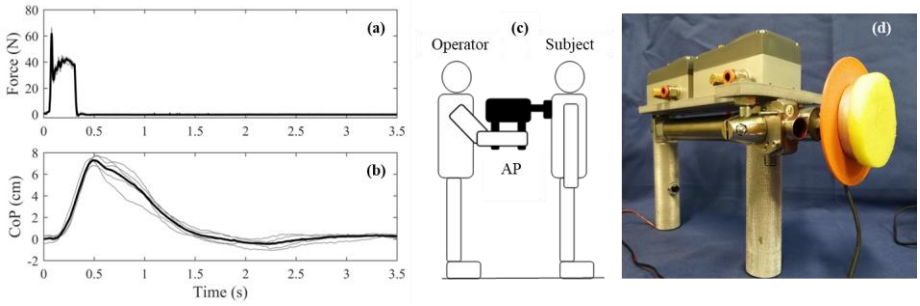

Fig. 1. Force (a) and CoP (b) signals for 10 Ns stimuli. Each plot shows 5 consecutive stimuli and the average signal in bold line. (c) Set-up of a trial, AP is the automatic perturbator (d).

2.2 Single-link and double-link inverted pendulum models

The segmented experimental data were used to fit two models for postural control based on inverted-pendulum formulation. A single (SIP) and a double (DIP) link models have been implemented in MATLAB-Simulink® to assess the dynamics of the human body in perturbed balance conditions. The non-linear analytical description of the plant has been considered in both cases, differently from the linearized version that is commonly used in similar works [14,16,17], to take into account those postural responses whose magnitude does not fall in the small displacement hypothesis. Figure 2 shows a representation of the free-body diagrams used to derive the mathematical formulation of the dynamics of both models.

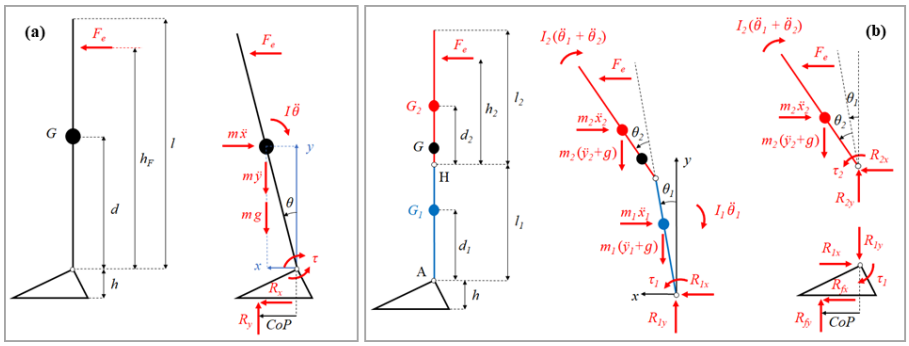

Fig. 2. Free-body diagrams for SIP (a) and DIP (b) models.

The diagrams clearly show the role of the correcting torques τ_i at each joint that are critical to achieve the stabilization of the system. Each torque has been modelled as the sum of a passive (intrinsic) and an active contribution, the former being dependent on the constraints and the visco-elastic behavior of tissues surrounding the joint, the latter being the result of the neuro-muscular control performed by the central nervous system (CNS) along with the afferences provided by the sensory systems through their respective feedback paths. In particular, the passive control can be generally described by the

sum of an elastic and a viscous term, whereas the active control is often implemented as a delayed, proportional-derivative (PD) action [15,17]. The torques included in SIP and DIP models have been implemented according to this approach, which requires the knowledge of the rotation angles and angular velocity at each joint. That information is part of the dataset that the CNS handles when posture is adjusted in quiet standing or during and after a perturbation. To account for errors in such estimation from the CNS, pink noise has been included in the model and tuned according to the literature (magnitude = $4 \cdot 10^{-3}$ rad [17]). The time delay setting for the active control action is necessary to take into account the finite response time of CNS coordinating the musculoskeletal system in the development of the postural reaction. Finally, as suggested by previous works [18], the muscle activation dynamics has been implemented by means of a second order transfer function (ω_n=15.7 rad/s, β=0.7) in series with the neural controller to filter out the high-frequency components of the controller output that are not compatible with the dynamics of the musculoskeletal system.

Some authors suggest the adoption of a term proportional to the acceleration within the active control logic when muscle activation dynamics is considered [19,20]. This approach has been tested in the SIP model, however it did not seem to be reasonable for the application considered. This result will be discussed later and motivated the exclusion of acceleration-related terms in the active control for the DIP model. In the latter, additional (indirect) terms considering the coupling between the two segments were added, as shown in [17], that link the torque at one joint to the rotation and angular velocity occurring at the other joint. A scheme reporting the general configuration of balance control system as implemented in the current work is presented in Fig. 3.

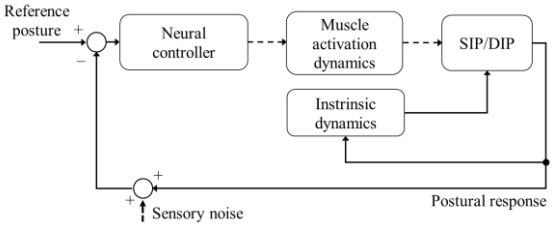

Fig. 3. Modeling of postural control system.

2.3 Parametric identification of balance control models

Optimization techniques for the parametric identification of SIP and DIP models have been investigated to achieve the best fit with the experimental dataset discussed in Section 2.1. A nonlinear least-squares solver (*lsqnonlin* in MATLAB®) has been selected as an adequate tradeoff between computational time and goodness of fit. This method requires an initial guess of the unknown parameters as input, that were derived from previous works [8], and it enables the possibility of setting lower and upper boundaries for each parameter. These limits were selected as large as possible to avoid over-constrained optimization, but still they helped in avoiding unrealistic sets of parameters (e.g., negative time delays) that could potentially lead to not feasible local minima of

the objective function. The latter was designed as the root-mean-square error (RMSE) between the average CoP signal measured during experimentation (CoP_e) and the one predicted by the model (CoP_m).

Before the optimization could be performed, the body mass and height of each subject were used to estimate the anthropometric parameters required by the models according to the formulation presented in the literature [21]. The point of application of the perturbation was set at the same height measured during trials (T4-T5 level), while its magnitude was set equal to the force signal averaged over 5 consecutive stimuli.

Due to the different formulations, the parameters included in the optimization algorithm were different between SIP and DIP models. Regarding SIP model, the active control proportional K_p and derivative K_d terms, the time delay T_d, the acceleration-proportional gain K_a, and the passive viscous gain B were subjected to optimization, whereas the passive elastic gain K was set to the 60 % of the critical stiffness of the ankle joint [22]. The same logic was applied to the DIP model, leading to the following set of parameters to optimize (1 refers to the ankle joint, 2 refers to the hip joint): the active control gains K_{p11}, K_{d11}, K_{p22}, K_{d22}; the time delays T_{d1} and T_{d2}; the passive viscous gains B_1 and B_2. The indirect terms of the active control action (K_{pij}, K_{dij}) were fixed and set according to the literature [17], while the passive elastic gains K_1 and K_2 were respectively set to the 60 % and to the 100 % of the respective joint critical stiffness, in agreement with the literature [22].

The optimization was performed separately for each subject and for each impulse level (6 Ns and 10 Ns). Each simulation led to an optimal set of parameters and to a corresponding value of RMSE between experimental and estimated CoP signals.

3 Results and Discussion

Figure 4a-c shows an example of the simulation outcomes on a single subject. Figure 4d shows the RMSE normalized with the maximum of CoP_e (NRMSE) for each subject and for both SIP and DIP models, considered as a metrics for goodness of fit.

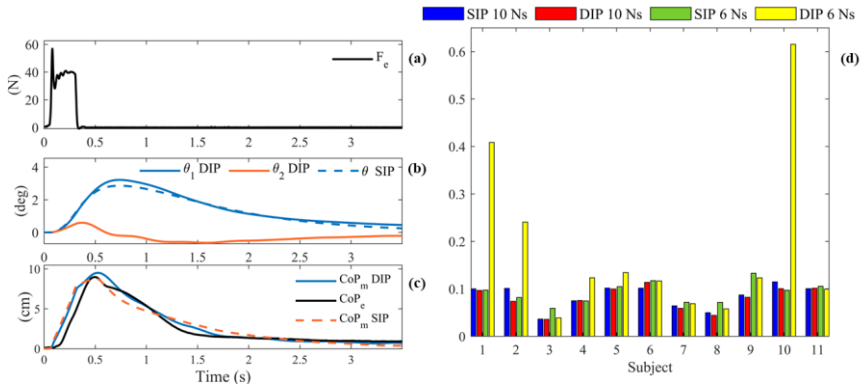

Fig. 4. Force signal (a), rotation angles (b) and CoP (c) fit for a single subject in SIP and DIP models. (d) Normalized RMSE values (NRMSE) for all subjects tested.

A qualitative assessment of fitting accuracy for a specific subject can be observed by the curves shown in Fig. 4c. In this particular case, the RMSE values obtained for both SIP and DIP models were lower than 5 mm, with the latter performing slightly better. This result was not confirmed for all the subjects as shown by data presented in Fig. 4d, since fitting for the DIP model at 6 Ns impulse level was sub-optimal for three subjects (#1, #2 and #10). This outcome may depend on multiple factors: (1) *lsqnonlin* algorithm performs local optimization, therefore the minimum of the objective function might be elsewhere; (2) low level impulse perturbations might evoke small oscillations in those subjects that compromise the usage of a double-link model. The latter hypothesis is motivated by the fact the DIP model still fits correctly in those subjects for 10 Ns perturbations. However, in-vivo data about kinematics or muscle activation would be necessary to confirm this deduction.

The values of optimized parameters obtained for both models are shown in Fig. 5.

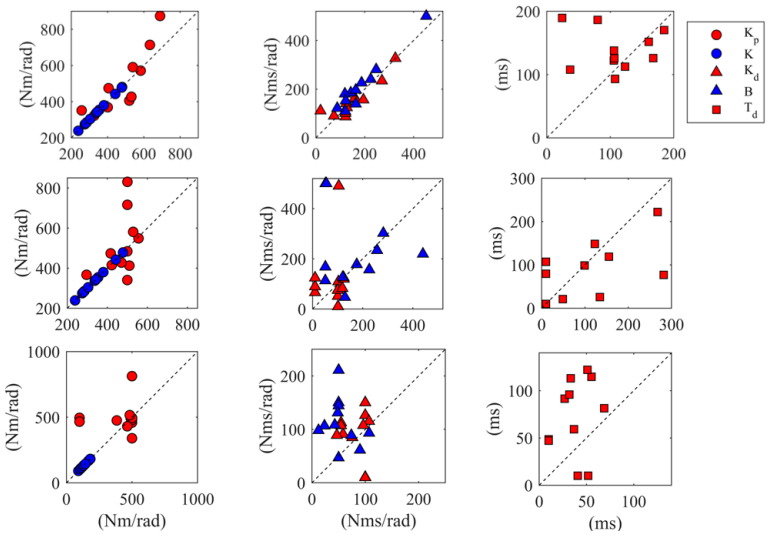

Fig. 5. Balance control parameters obtained after optimization: SIP model (top); DIP model, ankle joint (center); DIP model, hip joint (bottom). For each plot, *x*-axis presents the parameters obtained at 6 Ns, *y*-axis shows the corresponding values obtained at 10 Ns.

Only K_a (acceleration-proportional feedback in SIP model) was not included in the figure since it was forced to the lower boundary (0 Nms^2/rad) by the optimization algorithm for most of the subjects. This result is in contrast with the findings of some authors in the literature [20], however this might be explained by the significantly different features of the perturbation considered. In our work, the direct application of an impact force to the body of the subject causes a sudden increase of the body acceleration that is likely superior to the one considered in previous works. Therefore, the implementation of an acceleration-proportional feedback results in an overestimation of the control torque that does not allow accurate fit of the model. Data presented in Fig. 5 show quite a large variability of the optimized parameters among the different subjects,

nonetheless they are coherent with similar results presented in the literature [8,17,20]. Those differences might be related to inter-subject variability and could be in some way considered for a subject-specific characterization of postural control. However, further work has to be done to assess the robustness and physical or clinical significance of these parameters.

Finally, the same set of parameters obtained at the lower level (6 Ns) was used for simulating the behavior of the system when subjected to higher impulse level (10 Ns) perturbations, to investigate the ability of each tuned model to predict the postural response without falling into unrealistic behavior or instability. Figure 6 shows the results of these simulations, in which ΔRMSE was used as an indicator of the worsening in the quality of fit.

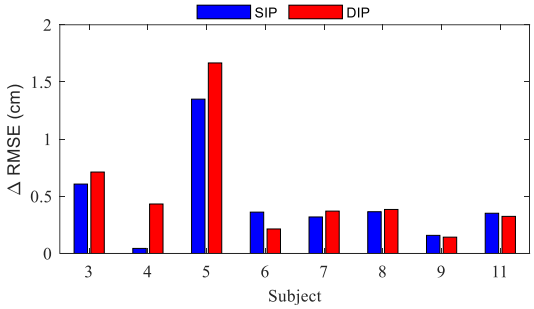

Fig. 6. Increase of residuals (ΔRMSE) for SIP and DIP models by selecting the sub-optimal configuration of control parameters. The results refer to 10 Ns impulse level.

For each subject, this parameter was calculated as the difference between the RMSE values respectively obtained by choosing the sub-optimal (estimated for the 6 Ns impulse level) and the optimal (estimated for the 10 Ns impulse level) sets of parameters. The outlier highlighted in Fig. 4d were excluded from this analysis. As shown in Fig. 6, the increased variance of the residuals for sub-optimal configuration of the control parameters was still lower than 5 mm for most of the subjects. Only two subjects (#3 and #5) showed large ΔRMSE due to significant differences between the sub-optimal and the optimal sets of control parameters provided by the algorithm. No significant difference was observed by comparing SIP and DIP results. This result provided a preliminary validation of the methodology and confirmed that both models, after tuning, were able to predict the postural response with a good level of accuracy for most of the subjects considered.

4 Conclusion

This work showed the application of a nonlinear optimization technique to parametric identification of postural control models. Those were fit to experimental data obtained during dynamic posturographic analyses performed with a custom-made automated perturbation device, which was able to exert perturbations with controlled impulse level. The accuracy of fitting was good for most of the subjects tested, leading to a preliminary validation of the methodology and to a set of optimized models that could

effectively predict the postural reactions in terms of CoP displacement over the base of support.

Compared to the previous work from the authors [11], the muscle activation dynamics implementation allowed for smoother CoP behavior in line with the measured signal, whose component frequencies are less than 20 Hz. Moreover, the identification of passive elastic and viscous gains unique for each subject allows for taking into account the influence of the anthropometric characteristics within the passive contribution. In this way, the active contribution should be influenced just by different postural control strategies. Finally, a double-link model has been developed to consider a hip strategy that could play a significant role, especially in response to greater impulses. However, neither SIP nor DIP model has proven to be indisputably optimal in terms of quality of fitting, hence their suitability to predict the correct behavior of postural control system remains under discussion. Of course, they allow for different observations since kinematics and dynamics variables refer to systems with single (SIP) or multiple (DIP) degrees of freedom. Therefore, the choice of the optimal model surely depends on the entity of the research questions to be answered.

Parametrized models of balance control can help in the investigation of the mechanisms and strategies developed to maintain the equilibrium, due to the simplified yet detailed description they allow of postural control system. The implementation of optimized postural control models can support the physical interpretation of parameters collected by experimentation (as the maximum CoP displacement, or the latency between perturbation and response) and improve the understanding of how those parameters are influenced by the characteristics of the subjects in a wider scenario than the one that can be feasibly investigated with experimental trials. However, it is fundamental to obtain good fitting with experimental data to consider a model reliable and accurate enough. In this sense the outcomes of our study are promising but, to further improve the quality of the results, future work should consider: (1) adding sensory feedback pathways to the models; (2) implementing more sophisticated models for neural controller, as suggested by recent literature [23,24]; (3) testing global optimization techniques to improve the goodness of fit; (4) expanding the experimental dataset.

References

1. Loram, I., Lakie, M.: Direct measurement human ankle stiffness during quiet standing: the intrinsic mechanical stiffness is insufficient for stability in most subjects. The Journal of Physiology, 545(3), 1041–1053 (2002).
2. Casadio, M., et al.: Direct measurement of ankle stiffness during quiet standing: implications for control modelling and clinical application. Gait & Posture, 21(4), 410–424 (2005).
3. Vlutters, M., et al.: Direct measurement of the intrinsic ankle stiffness during standing. Journal of Biomechanics, 48(7), 1258–1263 (2015).
4. Diener, H.C., et al.: Influence of stimulus parameters on human postural responses. J Neurophysiol, 59(6), 1888–1905 (1988).
5. Potocanac, Z., et al.: A robotic system for delivering novel real-time, movement dependent perturbations. Gait & Posture, 58, 386–389 (2017).

6. Robinson, C.J., et al.: Design, control, and characterization of a sliding linear investigative platform for analyzing lower limb stability (SLIP-FALLS). IEEE Transactions on Rehabilitation Engineering, 6(3), 334–350 (1998).
7. Grassi, L., et al.: Quantification of postural stability in minimally disabled multiple sclerosis patients by means of dynamic posturography: an observational study. Journal of NeuroEngineering and Rehabilitation, 14, 4 (2017).
8. Davidson, B.S., et al.: Neural control of posture during small magnitude perturbations: effects of aging and local-ized muscle fatigue. IEEE Transactions on Biomedical Engineering 58(6), 1546–1554 (2011).
9. Martinelli, A.R., et al.: Light touch modulates balance recovery following perturbation: from fast response to stance restabilization. Exp brain Res, 233(5), 1399–1408 (2015).
10. Maffiodo, D., et al.: Pneumo-tronic Perturbator for the Study of Human Postural Responses. Advances in Intelligent Systems and Computing, 980, 374–383 (2020).
11. Paterna, M., et al.: Center of pressure displacement due to graded controlled perturbations to the trunk in standing subjects: the force–impulse paradigm. European Journal of Applied Physiology, 122(2), 425–435 (2022).
12. Pacheco Quiñones, D., et al.: Automatic electromechanical perturbator for postural control analysis based on model predictive control. Applied Sciences, 11(9), 4090 (2021).
13. Dvir, Z. et al.: Linearity and repeatability of postural responses in relation to peak force and impulse of manually delivered perturbations: a preliminary study. European Journal of Applied Physiology, 120(6), 1319–1330 (2020).
14. Peterka, R.J.: Sensorimotor Integration in Human Postural Control. J Neurophysiol, 88, 1097–1118 (2002).
15. van der Kooij, H., et al.: Comparison of different methods to identify and quantify balance control. Journal of Neuroscience Methods, 145, 175–203 (2005).
16. van der Kooij, H., Peterka, R.J.: Non-linear stimulus-response behavior of the human stance control system is predicted by optimization of a system with sensory and motor noise. J Comput Neurosci, 30, 759–778 (2011).
17. Goodworth, A.D., Peterka, R.J.: Identifying mechanisms of stance control: A single stimulus multiple output model-fit approach. Journal of Neuroscience Methods, 296, 44–56 (2018).
18. Pasma, J.H., et al.: Changes in sensory reweighting of proprioceptive information during standing balance with age and disease. J Neurophysiol, 114, 3220–3233 (2015).
19. Welch, T.D.J., Ting, L.H.: A Feedback Model Reproduces Muscle Activity During Human Postural Responses to Support-Surface Translations. J Neurophysiol, 99, 1032–1038 (2008).
20. Pasma, J.H., et al.: Assessment of the underlying systems involved in standing balance: the additional value of electromyography in system identification and parameter estimation. Journal of NeuroEngineering and Rehabilitation, 14, 97 (2017).
21. Winter, D.A.: Biomechanics and Motor Control of Human Movement, Fourth Edition. John Wiley and Sons, 1–370 (2009).
22. Morasso, P., et al.: Quiet standing: The Single Inverted Pendulum model is not so bad after all. PLoS ONE, 14(3), e0213870 (2019).
23. Mengarelli, A., et al.: A Sliding Mode Control Model for Perturbed Upright Stance in Healthy Subjects. World Congress on Medical Physics and Biomedical Engineering 2018, IFMBE Proceedings 68/2, 719–724 (2019).
24. Wang, H., van den Bogert, A.J.: Identification of Postural Controllers in Human Standing Balance. Journal of Biomechanical Engineering, 143(4), 041001 (2021).